Available online at www.sciencedirect.com
SCIENCE DIRECT®
Journal of Environmental Radioactivity 68 (2003) 137–158
JOURNAL OF ENVIRONMENTAL RADIOACTIVITY
www.elsevier.com/locate/jenvrad

Radionuclides deposition over Antarctica

M. Pourchet [a], O. Magand [a,*], M. Frezzotti [b], A. Ekaykin [c], J.-G. Winther [d]

[a] *Laboratoire de Glaciologie et Géophysique de l'Environnement, CNRS, BP 96, 38402 St Martin d'Hères Cedex, France*
[b] *ENEA, CLIM-OSS, P.O. Box 2400, 00100 Rome A.D., Italy*
[c] *Arctic and Antarctic Research Inst., 38 Bering St., 199397 St. Petersburg, Russia*
[d] *Norwegian Polar Institute, Polar Environmental Centre, Tromso, Norway*

Received 17 June 2002; received in revised form 11 February 2003; accepted 21 February 2003

Abstract

A detailed and comprehensive map of the distribution patterns for both natural and artificial radionuclides over Antarctica has been established. This work integrates the results of several decades of international programs focusing on the analysis of natural and artificial radionuclides in snow and ice cores from this polar region. The mean value (37±20 Bq m^{-2}) of ^{241}Pu total deposition over 28 stations is determined from the gamma emissions of its daughter ^{241}Am, presenting a long half-life (432.7 yrs). Detailed profiles and distributions of ^{241}Pu in ice cores make it possible to clearly distinguish between the atmospheric thermonuclear tests of the fifties and sixties. Strong relationships are also found between radionuclide data (^{137}Cs with respect to ^{241}Pu and ^{210}Pb with respect to ^{137}Cs), make it possible to estimate the total deposition or natural fluxes of these radionuclides. Total deposition of ^{137}Cs over Antarctica is estimated at 760 TBq, based on results from the 90–180° East sector. Given the irregular distribution of sampling sites, more ice cores and snow samples must be analyzed in other sectors of Antarctica to check the validity of this figure.

Keywords: Radionuclides deposition; Flux; Antarctica

* Corresponding author. Tel.: +33-4-76-82-42-59; fax: +33-4-76-82-42-01.
E-mail address: magand@lgge.obs.ujf-grenoble.fr (O. Magand).

0265-931X/03/$ - see front matter © 2003 Elsevier Science Ltd. All rights reserved.
doi:10.1016/S0265-931X(03)00055-9

1. Introduction

Artificial radioisotopes resulting from atmospheric thermonuclear tests carried out between 1953 and 1980 were deposited in Antarctica after transport in the upper atmosphere and stratosphere, creating distinct radioactive reference levels in the snow. The dates of arrival and deposition in this polar region are well known and therefore provide a means to estimate Antarctic snow accumulation rates or describe air mass circulation patterns (Wilgain et al., 1965; Feely et al., 1966; Pourchet et al., 1983; Pourchet et al., 1997). The 1955 and 1965 radioactivity peaks provide two very convenient horizons for dating snow and ice layers and measuring accumulation. Special techniques have been developed over the last 40 yrs to detect and measure artificial and natural radionuclides present in the ice sheets (Picciotto and Wilgain, 1963; Delmas and Pourchet, 1977; Pinglot and Pourchet, 1979, 1994). In Antarctica, total beta counts remain the most frequent radioactivity measurement and are used to determine the average rate of snow accumulation (Picciotto and Wilgain, 1963; Lambert et al., 1977). Gamma profiles are also used for the determination of artificial and natural radionuclide fluxes in the region.

The total deposition of artificial radionuclides (mainly ^{137}Cs, ^{90}Sr and ^{3}H) and the flux of natural radionuclides (especially ^{210}Pb) has been estimated using snow samples from many Antarctic study areas (Pourchet et al., 1997), although simultaneous measurements of these major and complementary radionuclides in the same snow core are very rare. Snow and ice sheets on the Antarctic continent are not the only depositories of artificial and natural radionuclides deposited from the atmosphere over the south polar region. The deposition and flux of these radionuclides have also been measured in soils, plants and lake sediments, for example on the Antarctic Peninsula (Roos et al., 1994). A detailed profile of certain radionuclides has also been obtained for the Ross Ice Shelf (Koide et al., 1979).

In this work we have extended the previously available total deposition data by adding the results of a simultaneous analysis of ^{137}Cs, ^{210}Pb and ^{241}Pu in the same snow cores for about 30 stations located in various parts of Antarctica and a detailed profile of these three radionuclides for Vostok and Dome Concordia stations on the Antarctic plateau area. Key results of several decades of international programs and experiments focusing on artificial radionuclide analyses of snow or ice core samples in Antarctica are used in this paper.

In a previous paper (Pourchet et al., 1997), a distribution of artificial and natural radionuclides over Antarctica was proposed, based on ^{137}Cs, ^{210}Pb and ^{3}H data from snow and ice-core samples. In this work, additional radioactive analysis data are used to assess and extend the previous data, increasing the significance of statistical results and validating the distribution pattern previously proposed. The evidence of a strong correlation between radionuclides may make it possible to estimate the deposition and flux of one radionuclide from available data for another one. For ^{210}Pb, field data assess the possible double origin (unsupported and supported ^{210}Pb) of this terrigenous radionuclide in Antarctic snow and ice-core samples, a subject already discussed by Pourchet et al. (1997). Finally, the establishment of a distribution pattern for artificial and natural radionuclides, which constitute isotopic tra-

cers, can help us to understand the arrival and deposition of other artificial and natural tracers via atmospheric transport.

2. Material and methods

2.1. Study area and sample description

The snow and ice samples described in this paper were collected from cores or pits in different regions of the Antarctic continent, mainly in the 90–180° E sector from the Russian (Mirny to Vostok), Australian (Casey to Vostok), French (Dumont d'Urville to Dome C) and Italian (Talos Dome to Dome Concordia) transects. Ice-coring stations from other programs close to these transects were also used.

Twenty-eight stations previously analyzed for ^{137}Cs (Pourchet et al., 1997) were subject to new simultaneous ^{137}Cs, ^{210}Pb and ^{241}Pu measurements. The same analyses were also performed for 24 new locations (Table 1). For Vostok and Dome Concordia stations, detailed radionuclide deposition measurements were carried out (Table 2).

2.2. Analytical methods and procedure

Using a method developed by Delmas and Pourchet (1977), snow and ice core samples were melted, weighed, acidified and filtered on ion exchange paper, where all radionuclides were trapped. After drying, the filters were directly analyzed by gamma spectrometry using a low background germanium detector (Pinglot and Pourchet, 1994). Because of low activity, some samples were combined for radioactivity analysis (Pinglot and Pourchet, 1979, 1994). Most of the studied samples were analyzed at the LGGE laboratory in Grenoble. For high resolution gamma spectrometry, the analyzer was protected against all interfering ambient radioactivity, in particular using an anti-Compton device. This system provides a lower detection threshold, especially for the isotopes of interest such as ^{137}Cs (30.2 yrs), ^{210}Pb (22.3 yrs) and ^{241}Am (432.7 yrs), daughter of ^{241}Pu (14.4 yrs) (Pinglot and Pourchet, 1994, 1995; Pinglot et al., 1999).

Standard liquid ^{137}Cs, ^{210}Pb and ^{241}Am liquids from the CEA or Amersham laboratories (2% uncertainty at 95% of confidence level) were used to calibrate the detector. The analytical procedures were the same as those used for the snow samples. The accuracies for our measurements are about 20% for ^{137}Cs and ^{210}Pb and 50% for ^{241}Am. New determinations of ^{137}Cs for the 28 previously analyzed stations (Pourchet et al., 1997) confirm the accuracy of previous results (Fig. 1). The specific activities have been corrected for decay to the deposition time.

2.3. Measurements and determination of ^{241}Pu and ^{137}Cs

The ^{241}Pu and ^{137}Cs radionuclides constitute two well-known debris products of atmospheric thermonuclear tests between 1955 and 1980. ^{137}Cs is characteristic of both well-known reference layers in snow (1955 and 1965 peaks on beta profiles),

Table 1
Inventory of existing accumulation data, ^{137}Cs and ^{241}Pu density activities (Bq m^{-2}), and ^{210}Pb fluxes (Bq m^{-2} yr^{-1}) measured and calculated in snow and ice-core samples of different zones of the Antarctic continent

Stations	Lat. S	Long. E	Elevation	10 m temperature	Snow accumulation	Deposition (Bq m^{-2})			^{210}Pb	Ref.
						^{137}Cs		^{241}Pu	flux deposition	
	(°)	(°)	(m)	(°C)	(kg m^{-2} yr^{-1})	(a)	(b)		(Bq m^{-2} yr^{-1})	
Ice cores										
M.M	77.83	167.00	20		160		164*	n.m.	n.m.	3
J9	82.37	191.33	50	−29.4	90		89	16	1.90	1
F9	84.4	189.00	50	−30.4	84	17	18	9	2.36	2
km105	67.58	93.70	1351		313	51	155	51	4.22	2
km260	68.77	94.47	2280	−33	69		44	n.m.	1.28	2
km325	69.3	95.02	2560	−37	140		95	36	5.60	2
km400	69.95	95.62	2760	−40	154		81	42	5.40	2
km200	68.25	94.08	1970	−29	271		181	99	4.48	2
VK631	72.22	96.62	3421		68	52	56	18	2.55	2
Komso	74.1	97.50	3498	−53.9	64	52	86	80	3.43	2
VK747	73.25	97.07	3270		84	40	48	29	2.26	2
VK14	78.45	106.84	3470	−55.4	23		52	34	1.20	2
VK17	78.45	106.84	3470	−55.4	19	35	38	28	2.66	2
Vostok (a)	78.45	106.84	3471	−55.4	23		58	n.m.	n.m.	2
Vostok (b)	78.45	106.84	3471	−55.4	23		109	49	1.93	2
DB	76.92	95.17	3400		32	174	153	40	1.09	2
BHD	66.73	112.83	1315		631	59	59	n.m.	5.37	2
BHDB	66.73	112.83	1315		631	81	67	n.m.	4.49	2
GC38	70.44	111.74	2524	−38.9	121	50	59	39	1.74	2
GC40	71.17	111.36	2695	−43.6	126	55	46	23	3.52	2
GC47	73.70	110.20	3046	−52.1	45	36	27	n.m.	1.85	2
GD03	69.00	115.48	1832	−29.4	476	78	83	n.m.	3.45	2

(*continued on next page*)

Table 1 (*continued*)

Stations	Lat. S	Long. E	Elevation	10 m temperature	Snow accumulation	Deposition (Bq m^{-2})			^{210}Pb	Ref.
						^{137}Cs		^{241}Pu	flux deposition	
	(°)	(°)	(m)	(°C)	(kg m^{-2} yr^{-1})	(a)	(b)		(Bq m^{-2} yr^{-1})	
GD12	68.98	126.93	2170	−32.6	350	95	103	n.m.	3.77	2
GD15	69.00	130.81	2150	−33.3	356	100	107	n.m.	7.51	2
GF01	68.50	110.85	1800	−28.7	367	63	60	n.m.	3.63	2
GF04	68.53	107.24	2120	−32.7	293	46	62	n.m.	2.33	2
GM13	73.17	110.45	2960	−52.9	65		56	30	1.57	2
JRF	64.25	302.25	1690	−13.4	163	32	25	19	3.58	2
JRG	64.25	302.25	1350	−11.3	236	40	45	n.m.	4.57	2
PS (a)	90.00	90.00	2800	−50.7	80		67	56	1.91	2
PS (b)	90.00	90.00	2800	−0.7	80	53	53	37	1.64	2
New Byrd	80.00	240.00	1500		180		131*	n.m.	n.m.	3
R. Boudoin	70.43	24.32	20		400		195*	n.m.	n.m.	3
2-11-279	82.90	18.20	2610	−49.2	36		26*	n.m.	n.m.	3
1-15-415	85.20	1.60	2630	−48.6	61		45*	n.m.	n.m.	3
1-13-370	85.80	8.70	2690	-50	42		29*	n.m.	n.m.	3
1-10-275	86.60	30.60	2860	−47.9	55		33*	n.m.	n.m.	3
2-0-0	82.10	55.10	3720		31		21*	n.m.	n.m.	3
Livingston Is.	62.67	299.62	265	−4	681		16*	n.m.	n.m.	4
D.Du	66.70	139.80	43	−10.7	140		90*	n.m.	n.m.	5
A3	66.69	139.82	190	−14.3	220		114*	n.m.	n.m.	5
D9	66.70	139.82	223	−15	250		119*	n.m.	n.m.	5
D12	66.70	139.78	246	−15.3	350	63	74	n.m.	6.32	2

Table 1 (*continued*)

Stations	Lat. S	Long. E	Elevation	10 m temperature	Snow accumulation	Deposition (Bq m^{-2})			^{210}Pb	Ref.
						^{137}Cs		^{241}Pu	flux deposition	
	(°)	(°)	(m)	(°C)	(kg m^{-2} yr^{-1})	(a)	(b)		(Bq m^{-2} yr^{-1})	
D23	66.73	139.62	556	−17.5	440		88	n.m.	n.m.	4
D26	66.77	139.55	589	−17.9	275	44	54	42	5.55	2
D33	66.80	139.43	690	−18.3	139	26	39	50	4.04	2
D42	66.99	139.11	1028	−22	320	65	74	57	4.83	2
D43	67.06	139.01	1143	−22.6	240	52	55	28	7.28	2
D45	67.22	138.83	1353	−24	420		158*	n.m.	n.m.	6
D47	67.39	138.64	1524	−25.8	260	78	73	50	4.55	2
D50	67.62	138.33	1709	−27.6	240		64*	n.m.	n.m.	6
D53	67.86	137.99	1898	−29.8	360		125	n.m.	n.m.	4
D55	68.03	137.78	1995	−31.1	70	20	19	n.m.	0.82	2
D59	68.34	137.31	2228	−34.3	320		113*	n.m.	n.m.	6
D60	68.45	137.20	2291	−36.3	260		89	n.m.	n.m.	2
D66	68.94	136.49	2357	−38.8	200		113**	n.m.	n.m.	8
D72	69.44	135.76	2412	−41.2	230		59*	n.m.	n.m.	6
D80	70.02	134.82	2487	−41.4	240	92	95	36	5.51	2
D100	71.56	131.97	3100	−46.3	130		52*	n.m.	n.m.	5
D120	73.06	128.74	3280	−52.3	80		32*	n.m.	n.m.	5
DC (a)	74.64	124.17	3240	−53.5	32		43	22	1.13	2
DC (b)	74.64	124.17	3240	−53.5	32		47	16	1.07	2
Concordia	75.11	123.32	3232		28		36	13	0.44	2
Datsin Gangotri	70.00	12.00	20		135		74*	n.m.	n.m.	7
EPICA A	74.90	3.83	1520	−25.6	135		60	n.m.	n.m.	9, 10
B	72.13	3.17	2044	−28.1	171		44	n.m.	n.m.	9, 10

Table 1 (*continued*)

Stations	Lat. S	Long. E	Elevation	10 m temperature	Snow accumulation	Deposition (Bq m^{-2})			^{210}Pb	Ref.
						^{137}Cs		^{241}Pu	flux deposition	
	(°)	(°)	(m)	(°C)	(kg m^{-2} yr^{-1})	(a)	(b)		(Bq m^{-2} yr^{-1})	
C	72.26	2.89	2400	−30.3	123		62	n.m.	n.m.	9, 10
D	72.51	3.00	2610	−34.3	116		66	n.m.	n.m.	9, 10
E	72.67	3.66	2751	−36.9	59		68	n.m.	n.m.	9, 10
F	72.86	4.36	2840	−38.5	24		32	n.m.	n.m.	9, 10
G	73.04	5.04	2929	−40.1	30		38	n.m.	n.m.	9, 10
H	73.39	6.46	3074	−42.7	46		66	n.m.	n.m.	9,10
I	73.72	7.94	3174	−44.6	53		78	n.m.	n.m.	9, 10
J	74.04	9.49	3268	−46.3	52		82	n.m.	n.m.	9, 10
K	74.36	11.10	3341	−47.8	44		68	n.m.	n.m.	9, 10
L	74.64	12.79	3406	−49.3	41		62	n.m.	n.m.	9, 10
M	74.99	15.02	3453	−51.3	45		94	n.m.	n.m.	9, 10
CV	76.00	−8.05	2399	−38.6	67		83	n.m.	n.m.	9, 10
CM2	76.10	−13.16	362	−17.4	220		134	n.m.	n.m.	9, 10
NARE E	72.98	1.12	1817		50		46	n.m.	n.m.	10
F	73.10	−0.46	1974		120		79	n.m.	n.m.	10
H	70.50	−2.46	52		480		56	n.m.	n.m.	10
I	71.51	1.18	600		60		27	n.m.	n.m.	10
K	70.76	0	50		220		56	n.m.	n.m.	10
GPS1	74.84	160.82	1192		48		24	n.m.	1.10	2
GPS2	74.64	157.50	1776		53		44	n.m.	1.72	2
M2	74.80	151.27	2308		51		48	n.m.	2.10	2
D2B	75.55	145.79	2454		69			n.m.	1.57	2
D2	75.62	140.63	2611		39		44	n.m.	n.m.	2

Table 1 (*continued*)

Stations	Lat. S	Long. E	Elevation	10 m temperature	Snow accumulation	Deposition (Bq m^{-2})			^{210}Pb	Ref.
						^{137}Cs		^{241}Pu	flux deposition	
	(°)	(°)	(m)	(°C)	(kg m^{-2} yr^{-1})	(a)	(b)		(Bq m^{-2} yr^{-1})	
D4B	75.60	135.83	2792		21		40	n.m.	n.m.	2
D6D	75.45	129.81	3024		22		53	n.m.	1.18	2
P8	77.20	155.50	2492		2		16	n.m.	0.57	2
P10	76.64	147.36	2477		2.5		28	n.m.	0.36	2
P11	76.88	141.92	2626		1.6		24	n.m.	0.58	2
P12	77.54	137.02	2640		1.7		28	n.m.	0.74	2
Lichens (mean values)										
K.G.Is. (*n*=2)							96	41.7	5.095	11
Horsehoe							241	107	10.68	11
Living (*n*=5)							173.8	79	10.10	11
Mosses, grass, soils (mean values)										
K.G.Is. (*n*=6)							381.66	56	8.3	11
Living (*n*=5)							285	52	8.3	11
Sediment (mean values) (*n*=3)							348.33	94	4.5	11

The 10-m temperature corresponds to the value generally used to estimate the mean annual temperature for selected area. Global deposition of ^{137}Cs and ^{241}Pu are corrected for decay to the deposition time. Deposition times are respectively centered around 1957 for ^{241}Pu, and 1965 for ^{137}Cs. For ^{137}Cs values, the (a) data series gives the prior measurements and (b) data series, the new ^{137}Cs measurements. We have also to distinguish: ^{137}Cs deduced from ^{210}Pb flux calculations (*). ^{210}Pb flux is calculated from ^{210}Pb specific activities measurements (Bq kg^{-1}), and application of relations (3) and (6) (see text). ^{137}Cs deduced from ^{90}Sr measurements (**) using the ratio ^{90}Sr/^{137}Cs=1.6. n.m., not measured. Ref. 1=Koide et al. (1979); 2=this work; 3=Crozaz (1967, 1969); 4=Pourchet et al. (1997); 5=Sanak (1983); 6=Lambert et al. (1983); 7=Nijampurkar and Rao (1993); 8=Bendezu (1978); 9=Isaksson et al. (1999); 10=private com. (cf Isaksson); 11=Roos et al. (1994).

Table 2
Distribution of ^{137}Cs and ^{241}Pu flux deposition (Bq m^{-2}), and ^{210}Pb specific activities (Bq kg^{-1}) in ice core samples from Vostok and Dôme Concordia Stations

No.	Mean depth (cm)	^{137}Cs (Bq m^{-2})	^{241}Pu (Bq m^{-2})	^{210}Pb (Bq kg^{-1})
Vostok				
1	5	0	0	0.0682 ± 0.0136
2	15	0	0	0.1158 ± 0.0232
3	25	0	0	0.0836 ± 0.0168
4	35	0	0	0.1074 ± 0.0214
5	45	0	0	0.0543 ± 0.0108
6	55	0	0	0.0463 ± 0.0092
7	65	0	0	0.0439 ± 0.0088
8	75	0	0	0.0824 ± 0.0164
9	85	0.14 ± 0.03	0	0.0626 ± 0.0126
10	95	0.12 ± 0.02	0	0.0378 ± 0.0076
11	105	0.21 ± 0.04	0	0.0532 ± 0.0106
12	115	0.27 ± 0.05	0	0.0372 ± 0.0074
13	125	0.21 ± 0.04	0	0.0560 ± 0.0112
14	135	0.23 ± 0.05	0	0.0420 ± 0.0084
15	145	0.87 ± 0.17	0	0.0443 ± 0.0088
16	155	2.05 ± 0.41	0	0.0348 ± 0.0070
17	165	3.28 ± 0.66	0	0.0388 ± 0.0078
18	175	5.19 ± 1.04	0	0.0275 ± 0.0054
19	185	9.43 ± 1.88	1.92 ± 0.96	0.0293 ± 0.0058
20	195	11.87 ± 2.37	2.16 ± 1.08	0.0213 ± 0.0042
21	205	15.15 ± 3.03	2.55 ± 1.23	0.0299 ± 0.0060
22	215	12.59 ± 2.52	4.31 ± 2.15	0.0389 ± 0.0078
23	225	6.06 ± 1.12	1.50 ± 0.75	0.0300 ± 0.0060
24	235	5.69 ± 1.14	1.35 ± 0.67	0.0442 ± 0.0088
25	245	11.14 ± 2.23	5.61 ± 2.80	0.0254 ± 0.0050
26	255	18.40 ± 3.68	20.73 ± 10.37	0.0215 ± 0.0042
27	265	5.32 ± 1.06	7.59 ± 3.79	0.0290 ± 0.0058
28	275	0.56 ± 0.11	0.78 ± 0.39	0.0309 ± 0.0062
Dôme Concordia				
1+2	10	0	0	0.0170 ± 0.0034
3+4	30	0	0	0
5	45	0	0	0
6+7	60	0	0	0.0362 ± 0.0072
8	75	0.010 ± 0.002	0	0.0223 ± 0.0045
9	85	0	0	0
10	95	0	0	0.0129 ± 0.0026
11+12	110	0	0	0.0216 ± 0.0043
13	125	0	0	0.0148 ± 0.0030
14	135	0.020 ± 0.004	0	0.0245 ± 0.0049
15	145	0	0	0.0214 ± 0.0043
16	155	0	0	0.0153 ± 0.0031
17	165	0	0	0.0169 ± 0.0034
18+19	180	0.10 ± 0.02	0	0.0107 ± 0.0021

(*continued on next page*)

Table 2 (*continued*)

No.	Mean depth (cm)	^{137}Cs (Bq m^{-2})	^{241}Pu (Bq m^{-2})	^{210}Pb (Bq kg^{-1})
20	195	0.07 ± 0.01	0	0.0116 ± 0.0023
21	205	0.19 ± 0.04	0	0.0133 ± 0.0027
22	215	0.11 ± 0.02	0	0.0131 ± 0.0026
23	225	0	0	0
24	235	0.24 ± 0.05	0	0
25	245	0.39 ± 0.08	0	0
26	255	0.24 ± 0.05	0	0.0094 ± 0.0019
27	265	0.69 ± 0.14	0	0.0124 ± 0.0025
28	275	1.53 ± 0.31	0	0.0183 ± 0.0037
29	285	2.45 ± 0.49	0	0.0069 ± 0.0014
30	295	2.09 ± 0.42	0	0.0151 ± 0.0030
31	305	0.78 ± 0.16	0	0.0154 ± 0.0031
32	315	1.45 ± 0.29	0	0
33	325	5.81 ± 1.16	0	0
34	335	3.99 ± 0.79	0	0.0100 ± 0.0020
35	345	2.08 ± 0.41	0	0.0167 ± 0.0033
36	355	1.91 ± 0.38	0	0.0182 ± 0.0036
37	365	1.59 ± 0.32	0	0.0165 ± 0.0033
38	375	1.27 ± 0.25	0	0
39	385	1.61 ± 0.30	2.21 ± 1.10	0.0079 ± 0.0016
40	395	6.49 ± 1.30	10.91 ± 5.45	0.0240 ± 0.0048
41	405	0.75 ± 0.15	0	0.0195 ± 0.0039
42	415	0	0	0.0099 ± 0.0020
43	425	0	0	0.0097 ± 0.0019

^{137}Cs and ^{241}Pu flux values are decay-corrected to the deposition time (1957 for ^{241}Pu; 1965 for ^{137}Cs). ^{210}Pb concentrations correspond to direct values, at the time measurements (respectively 1999 and 2001). Because of ^{210}Pb half-life (22.3 yrs), there is no decay-correction influence on measured specific activities between 1999 and 2001 values.

corresponding to the arrival and deposition of artificial radionuclides in Antarctica. ^{241}Pu, on the other hand, is prominent mainly in the older reference level (1955). Indeed, the Yvy and Castles series of tests conducted in 1953 produced more ^{241}Pu than the atmospheric thermonuclear tests in the sixties. This radionuclide therefore makes it possible to distinguish between the two test series.

The activity of ^{137}Cs was directly estimated and calculated from high resolution gamma spectrometry results. To estimate the activity of the ^{241}Pu radionuclide (pure alpha emitter), characterized by a short half-life (14.4 yrs), we used the gamma emission of its daughter ^{241}Am, presenting a long half-life (432.7 yrs). ^{241}Pu activity is calculated from the ^{241}Am measurement using a zero value for the daughter at the time of explosion (t_0).

At time t, the growth of ^{241}Am is calculated using the following equation:

$$^{241}\mathrm{Am}(t) = {}^{241}\mathrm{Pu}(t_0)\,[e^{-\lambda 1 * t} - e^{-\lambda 2 * t}]/[(\lambda_2/\lambda_1) - 1] \quad (1)$$

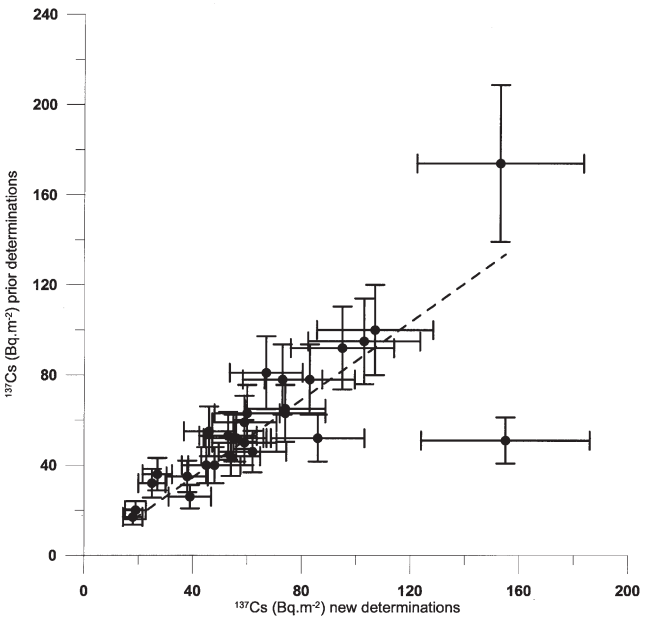

Fig. 1. ^{137}Cs new density activities versus ^{137}Cs previous data (Pourchet et al., 1997) measured in snow and ice samples for 28 ice-coring stations. Density activities, decay-corrected to deposition time, are expressed in Bq m^{-2}. Accuracies for ^{137}Cs are about 20% (see error bars).

where λ_1 (0.069 yr^{-1}) and λ_2 (0.00231 yr^{-1}) are the radioactive constants for ^{241}Pu and ^{241}Am respectively.

Based on the radioactive decay law, the maximum activity of ^{241}Am occurs 32 yrs after ^{241}Pu production:

$$t_m = [1/(\lambda_2 - \lambda_1)]\log_{10}(\lambda_2/\lambda_1) \quad (2)$$

where t_m is time of maximum activity of the daughter radionuclide, ^{241}Am in this case. t_m is expressed in yrs.

In agreement with detailed profiles of radionuclide deposition on the Ross Ice Shelf (Koide et al., 1979) and at Vostok and Dome Concordia (this work), and also with the well documented arrival dates of total beta peaks (Jouzel et al., 1979), we have assumed that ^{137}Cs and ^{241}Pu deposition are respectively centered around 1965 and 1957. In fact, we have to clearly distinguish between the time of maximum activity (1955 and/or 1965), well-known in radioactive fallout over Antarctica, and the time of the mean deposition of each radionuclide ^{137}Cs and ^{241}Pu. Indeed, the ^{241}Pu profile in one ice-core sample showed a maximum activity in 1955, but the mean value of the total deposition is considered to be centered around 1957. For ^{137}Cs, the maximum activity and the mean of the total deposition occur simultaneously, i.e. in 1965. Tables 1 and 2 summarize ^{137}Cs, ^{210}Pb and ^{241}Pu activities (expressed in Bq m^{-2}) found in the different samples. Note that the absence of activity values for the ^{241}Pu nuclide in some cases does not indicate the total absence

of this radionuclide in the snow. In these cases, the activity of ^{241}Pu is simply so low that it cannot be distinguished due to the detection limit of the analyzer for the counting times used.

2.4. Measurements and determination of ^{210}Pb

Lead 210, a natural beta emitter, is a long-lived daughter nuclide (half-life 22.3 yrs) belonging to the Uranium 238 family (Picciotto and Crozaz, 1971). Its presence in the atmosphere is a result of the alpha radioactive decay of radon gas (^{222}Rn). Note that the atmosphere, via tropospheric and stratospheric circulation, is the major source of ^{210}Pb in Antarctica. The permanent ice over the Antarctic continent that prevents the escape of radon from geological substrates, the surrounding ocean without radon emanation and the time required for air masses to move from continental areas (source of radon emission) to south polar region all result in a low radon (and its daughter nuclide) concentration in Antarctica (Pourchet et al., 1997).

In this work, ^{210}Pb was directly analyzed by gamma spectrometry. The deposition of ^{210}Pb and the related natural fluxes are summarized in Tables 1 and 2.

The mean value of the continuous ^{210}Pb deposition flux (A_0 expressed in Bq m^{-2} yr^{-1}) can be estimated by:

$$A_0 = \lambda S/[\exp(-\lambda t_1) - \exp(-\lambda t_2)] \quad (3)$$

where λ is the ^{210}Pb radioactive decay constant ($\lambda = 0.03114$ yr^{-1}); S is the remaining activity of ^{210}Pb in the total core at the time of measurement, using the mean annual accumulation rate; this value is expressed in Bq m^{-2}; t_1 is the elapsed time (expressed in yrs) between core sampling and ^{210}Pb measurement; t_2 is the elapsed time (expressed in yrs) between deposition of the deepest part of the core analyzed and the ^{210}Pb measurement.

In this work, in order to estimate ^{210}Pb deposition flux, we have systematically chosen to analyze data between the first reference layer of 1955 and the top of the core (or sometimes a few meters below the top). This interval was previously the subject of total beta radioactivity measurements used to determine the mean annual accumulation.

3. Results

3.1. Comparison between prior and new ^{137}Cs determinations

As already pointed out, we carried out new ^{137}Cs determinations for 28 previously analyzed stations (Pourchet et al., 1997). For all 28 stations, old and new ^{137}Cs measurements are linked by the following equation:

$$Y \text{ (prior } ^{137}\text{Cs values)} = 0.8615\, X \text{ (new } ^{137}\text{Cs values)}\ R^2 = 0.91 \quad (4)$$

$$(n = 28)$$

where prior and new ^{137}Cs values are expressed in Bq m^{-2}.

However, a detailed analysis of the scatter plot of old ^{137}Cs vs. new ^{137}Cs shows two outlying pairs of measurements. After eliminating these pairs, the relation between old ^{137}Cs vs. new ^{137}Cs shows a linear correlation of 0.98. The relation is as follows:

$$Y\,(\text{prior } ^{137}\text{Cs values}) = 0.9225\,X\,(\text{new } ^{137}\text{Cs values}) \quad R^2 = 0.98 \quad (n = 26) \tag{5}$$

This trend confirms the validity of previous results (Pourchet et al., 1997) and that of the analytical procedure.

3.2. History and Vostok and Dome Concordia chronologies

The chronology of the arrival of undifferentiated or major artificial radionuclides is very well known in Antarctica. The first significant increase (peak intensity) of total beta radioactivity was observed in January 1955 (Picciotto and Wilgain, 1963; Vickers, 1963; Woodward, 1964; Wilgain et al., 1965) and corresponds to the arrival of the Yvy and Castles atmospheric thermonuclear tests, conducted in the Pacific Islands in November 1952 and March 1954, respectively. The continuation of high-yield bomb tests in the atmosphere, despite the nuclear moratorium in 1960, maintained the radioactivity of Antarctic precipitation at a significant level. The minimum fallout observed in 1961, was then followed by an increase reaching a maximum in 1964–1965 (Picciotto and Crozaz, 1971). The highest recorded total activity due to the American and U.S.S.R. test series arrived in January 1965 (Wilgain et al., 1965; Lambert et al., 1977; Jouzel et al., 1979). Note that the marked activity surge (highest intensity peak) in the 1955 reference layer with regard to total activity in 1964–1965 is due to a combination of several factors including the very high power of first detonation of the Castle test series, the southern hemisphere location of the test and the time of the year at which it was set off (rapid transfer into the atmosphere and to the ground).

The two reference layers were clearly identified in the Vostok ^{137}Cs profile at respectively 250–260 cm (88.3–92.0 cm w.e.) and 200–210 cm (70.1–73.7 cm w.e.) depths (Fig. 2a) and should be considered as two unambiguous references for dating ^{210}Pb and ^{241}Pu deposition. As we have already pointed out, ^{241}Pu deposition in Vostok is mainly concentrated in the 1955 layer. This is in accordance with Ross Ice Shelf ^{241}Am deposition (Koide et al., 1979), the $^{239+240}$Pu snow profile at Dome C (Cutter et al., 1979) and our results at Dome Concordia (Fig. 2b).

3.3. ^{210}Pb dating and origin

The mean annual accumulation for the 1955–1998 and 1965–1998 periods deduced from both reference levels are respectively 2.05 and 2.18 cm of water equivalent (w.e.). For the 1955–1998 period, the mean annual accumulation deduced from the radioactive decay of ^{210}Pb in the snow profile is 2.57 cm w.e. The conversion of

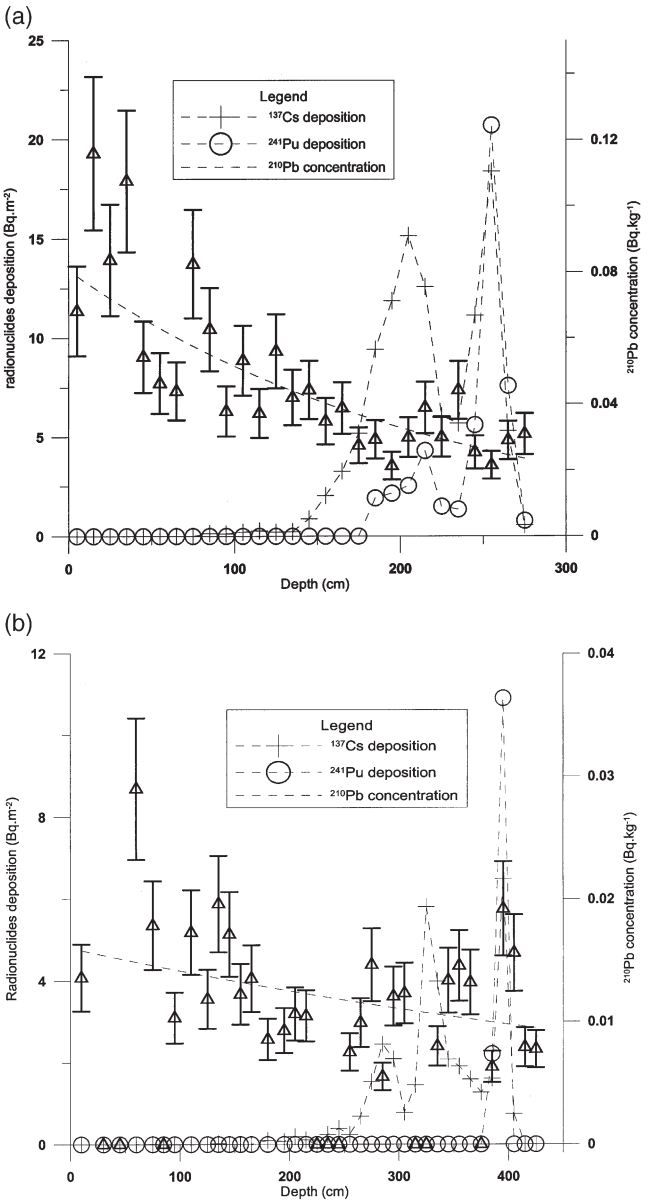

Fig. 2. ^{137}Cs, ^{241}Pu and ^{210}Pb profiles versus depth of two shallow Vostok (a) and Dôme Concordia (b) ice cores, with the 1955 and 1965 radioactive reference layers (indicated by an arrow). Radionuclides deposition (^{137}Cs and ^{241}Pu) are expressed in Bq m^{-2}, and ^{210}Pb specific activity, in Bq kg^{-1}. Depth is expressed in cm of snow equivalent.

real snow depths to water equivalents eliminates all distortion related to differences in the compaction of snow layers. The activity density profile of ^{210}Pb (Bq kg^{-1}) is therefore expressed as a function of the depth expressed in cm of water equivalent. For this estimation, we assumed a constant deposition flux of ^{210}Pb from the atmosphere to the snow, a closed system for lead following its deposition, and no changes in ^{210}Pb activity through exchanges by diffusion or percolation of melt water (Picciotto and Crozaz, 1971). This value is significantly higher than the absolute ^{137}Cs determination. Possible reasons for this discordance include the following factors:

(i) a change in the annual ^{210}Pb deposition flux;
(ii) a change in the annual snow accumulation;
(iii) part of the total ^{210}Pb (^{210}Pb$_t$) content in the snow coming from ^{210}Pb supported by long-life radionuclides of the ^{238}U family (^{210}Pb$_s$).

The first reason can be eliminated given the known constant ^{210}Pb deposition flux over the time period in question. Similarly, the second reason can be eliminated given the absolute dating provided on the basis of the 1955 and 1965 reference layers with respect to the surface.For the last reason, the ^{210}Pb dating, in all snow samples, must be calculated using ^{210}Pb excess (^{210}Pb$_e$) expressed in Bq kg^{-1} from:

$$^{210}\mathrm{Pb}_e = {}^{210}\mathrm{Pb}_t - {}^{210}\mathrm{Pb}_s \quad (6)$$

where ^{210}Pb$_e$ is the excess or unsupported ^{210}Pb activity produced in the atmosphere by radioactive decay of ^{222}Rn, ^{210}Pb$_t$ the total ^{210}Pb activity measured in snow samples and ^{210}Pb$_s$ the ^{210}Pb activity supported by long-life radionuclides of the ^{238}U family.

For the 1955–1998 period a similar value of the yearly average accumulation deduced from ^{137}Cs or ^{210}Pb is obtained when we apply a constant value of 9 mBq kg^{-1} to the ^{210}Pb$_s$. With this value, ^{210}Pb$_e$ and ^{210}Pb$_s$ are equal for a 65-year old snow sample. This result is consistent with a previous estimation based on ^{226}Ra measurements at Dome C, where the same activity for both parts of ^{210}Pb$_t$ was calculated for 60-year old snow (Pourchet et al., 1997). Note however that snow redistribution by wind should not be neglected as it can disturb snow and ^{210}Pb deposition over several yrs, and consequently the ^{210}Pb dating.

At Dome Concordia, the ^{137}Cs and ^{241}Pu profiles (Fig. 2b) are very similar to the Vostok profiles and give a mean annual accumulation of 3.2 cm w.e. since 1955. Even if the accuracy of the ^{241}Pu values is only about 50%, we obtain accurate mean annual accumulation values because the depth of corresponding reference layer is very precise. However, the ^{210}Pb profile is very disturbed and does not allow proper dating or an estimation of the unsupported ^{210}Pb$_e$.

3.4. Total deposition and fluxes of radionuclides

3.4.1. Radionuclide deposition and the ^{137}Cs/^{241}Pu relationship

For the whole studied deposition period (1955–1980), the total ^{137}Cs fallout over all the stations analyzed (Table 1) varies from 16 (P8 station) to 181 Bq m^{-2} (km

200), with a mean value of 64 ± 32 Bq m^{-2}. The median of 56 Bq m^{-2} lies 12.5% below the mean value, revealing an asymmetric distribution of ^{137}Cs, as observed in Pourchet et al. (1997). Some very high values from 200 km, R. Baudoin, M.M., DB, D45, D53, New Byrd and CM2 stations can be considered as outliers. A map of the deposition and distribution of ^{137}Cs over Antarctica for the whole deposition period (1955–1980) shows that radionuclide fallout is higher over coastal areas. We deliberately decided to describe the radionuclide distribution in the most documented and studied area in Antarctica, i.e. the 90–180° East sector (Fig. 3). Data from the other sectors of Antarctica cover shorter periods and would likely be insufficient to draw conclusions on a global radionuclide distribution law. Despite major scatter in individual values, classification of this data into several groups of accumulation rates clearly shows a positive correlation between ^{137}Cs deposition and accumulation. As well, we observe a discontinuity in the relation (Fig. 4) near an accumulation rate of 150 kg/m^2/year, indicating the possible existence of two radionuclide distribution laws. This discontinuity, already observed (Pourchet et al., 1997), lies between coastal areas and the polar plateau. The first classes, characterized by low accumulation rates and ^{137}Cs fall-out, correspond to the plateau area. The second group includes the sampling sites near the coast. Note that the leaching of radioactive aerosols is higher for sampling sites characterized by low accumulation rates (e.g. Antarctic plateau). Assuming that is possible to extrapolate ^{137}Cs flux values to zero accumulation, a "dry flux" of 43 Bq m^{-2} is obtained for ^{137}Cs, which is consistent with a previous estimation of "dry deposition" (Pourchet et al., 1997). Comparison of ^{137}Cs distribution in three latitudinal classes shows discontinuities in deposition. For 60–70°, 70–80° and 80–90° lat. S, mean ^{137}Cs deposition is respectively 77, 58 and 57

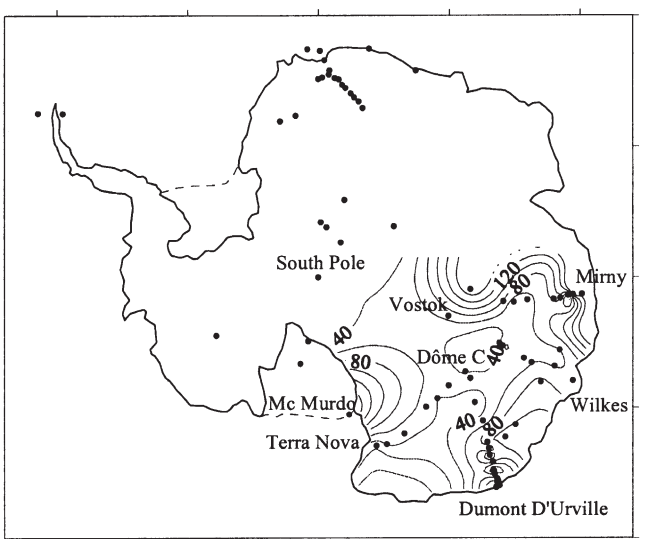

Fig. 3. Deposition and distribution Antarctic map ^{137}Cs (sector 90–180° East) for the whole deposition period 1955–1980.

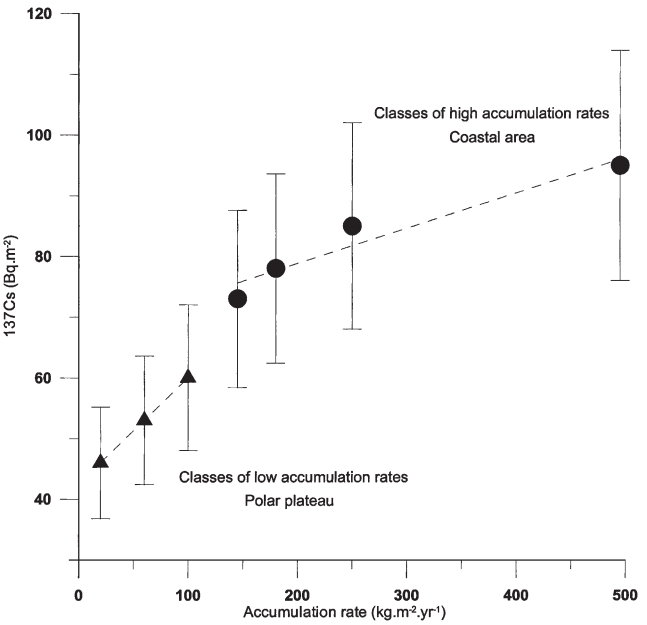

Fig. 4. Variation of total ^{137}Cs deposition versus accumulation rates in sector 90–180° East of Antarctica, and illustration of existence of two radionuclide distribution laws between coastal areas and polar plateau. Density activities values represent the 1955–2000 period. Radionuclide deposition is expressed in Bq m^{-2}, and accumulation rates in kg m^{-2} $year^{-1}$.

Bq m^{-2}. A clear change in ^{137}Cs deposition processes is observed close to the breaking slope on Antarctic plateau, near 80° lat. S.

The maximum deposition of ^{241}Pu is observed at 200 km, but many stations (57% of stations studies) are below the detection limit (between 5 and 10 Bq m^{-2}), depending on the counting time. The total fallout of ^{241}Pu over stations for which this radionuclide is detectable (Table 1), varies from 9 (F9 station) to 99 Bq m^{-2} (200 km), with a mean value of 37 ± 20 Bq m^{-2}. Regarding the ^{137}Cs distribution, the median value of ^{241}Pu, i.e. 36 Bq m^{-2}, is close to the mean value, demonstrating the symmetry of the distribution of this radionuclide. Nevertheless, given the large dispersion of values around the mean and the low number of results studied, we must be cautious when analyzing ^{241}Pu. Note also that the least squares method was used for statistical analysis and the linear best-fit regression was forced through the origin.

Considering only the stations for which ^{241}Pu is clearly detectable, i.e. 28 stations, ^{137}Cs and ^{241}Pu total deposition values are highly correlated (Fig. 5a) according to the following equation:

$$[^{241}\mathrm{Pu}] = 0.484\,[^{137}\mathrm{Cs}]\; R^2 = 0.92\; (n = 28) \tag{7}$$

This relationship is very close to that obtained from lichens (*Alectoria nigricans*

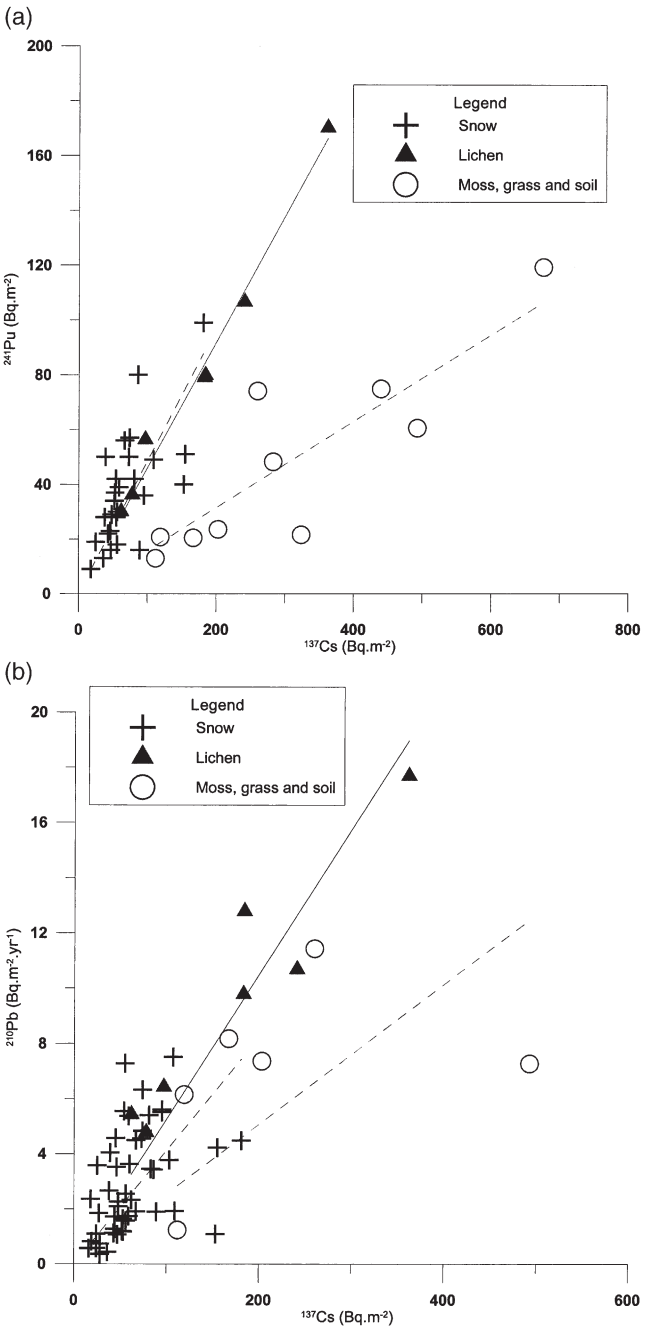

Fig. 5. ^{241}Pu versus ^{137}Cs deposition (a) and ^{210}Pb flux versus ^{137}Cs deposition (b) in different types of samples (snow, soils and lichens). Radionuclides deposition are both expressed in Bq m^{-2}, and ^{210}Pb flux deposition in Bq m^{-2} yr^{-1}.

species) collected on the Antarctic Peninsula area by Roos et al. (1994) (eight sampling stations):

$$[^{241}\mathrm{Pu}\,] = 0.454\,[^{137}\mathrm{Cs}\,]\;R^2 = 0.99\;(n = 8) \quad (8)$$

At the time of deposition, the mean $^{137}Cs/^{241}Pu$ ratio for total deposition is 1.9 for the snow stations and 2.3 for the lichens (Table 3). The detailed profiles of Vostok and Dome Concordia give similar values (2.2 and 2.7, respectively). This relative concordance between ^{137}Cs and ^{241}Pu is not observed on various types of moss and grass, sampled during the SWEDARP expedition, because of the effects of submergence and meltwater that alter the radionuclide ratios, as explained by Roos et al. (1994). Similarly, sediment samples collected on the Antarctic Peninsula show strong variations in the $^{137}Cs/^{241}Pu$ ratio and no relationship has been found. Normally sediments, like snow, are good accumulators of tracers (radionuclides in our case) and therefore could provide a $^{137}Cs/^{241}Pu$ ratio close to that observed in snow and lichen samples. However, the very low rate of sedimentation in the lakes concerned (30–100 cm to 1000 yr^{-1}) and the large surrounding snow fields delivering meltwater to the lakes explain the high variations (Roos et al., 1994).

3.4.2. Reference levels for the $^{137}Cs/^{241}Pu$ at Vostok and DC

The very large Pu ratios ($^{137}Cs/^{241}Pu$) observed during the early US test series are confirmed for Vostok station by the separate 1955 and 1965 peak ratios (respectively 0.9 and 5.9). Similar trends have previously been observed for the Ross Ice Shelf (Koide et al., 1979) but with different absolutes values. The 1965 value measured at Dome Concordia is too low for a significant evaluation of this ratio. With ^{241}Pu deposition centered at 1957, the maximum activity of ^{241}Am at the same level would occur 32 yrs later, i.e. in 1989. Due to its long half life, the relative importance of this radionuclide is increasing.

Table 3
Spatial variations of $^{137}Cs-^{241}Pu$ ratio in different Antarctic locations. and comparison of the calculated fission products relationships in different types of samples (snow, sediments, soils and lichens)

	$^{137}Cs/\ ^{241}Pu$						
	Snow stations	Vostok	Dome Concordia	J9 (1)	South Shetland Island (11)		
					lichens	moss, grass, soils	sediments
1955 peak		0.9	0.6	1.6			
1965 peak		5.9		9.2			
Mean value	1.9 (*n*=27)	2.2	2.7	5.4	2.3 (*n*=8)	7.1 (*n*=11)	5.9 (*n*=3)

The number of determinations (*n*) used to calculate the mean value are indicated in brackets. The bibliographic references for the station J9 (1) and the South Shetland Island (11) correspond respectively to Koide et al. (1979) and Roos et al. (1994) (see Table 1).

3.4.3. Mean $^{210}Pb/^{137}Cs$ ratio and relationship

The ^{210}Pb deposition flux ($^{210}Pb_f$) is linked to total ^{137}Cs deposition (Fig. 5b) by the relation:

$$[^{210}Pb_f] = 0.041\ [^{137}Cs]\ R^2 = 0.84\ (n = 49) \quad (9)$$

Compared to the $^{137}Cs/^{241}Pu$ relation, the $^{210}Pb/^{137}Cs$ ratios are very close for snow or ice-core samples and the lichens studied by Roos et al. (1994).

The good correlation between the different radionuclides suggests the creation of an undifferentiated radionuclide deposition (or flux) map over Antarctica. With this aim, we have calculated the equivalent ^{137}Cs deposition (Table 1) using all available ^{210}Pb or ^{90}Sr data.

4. Discussion

The proposed map is constructed using a constant ratio between the different radionuclides. This relationship does not take into account the differences in the fallout mechanisms for radionuclides observed elsewhere, for example the differences in the dry and wet deposition between ^{210}Pb, ^{90}Sr and ^{137}Cs (Pourchet et al., 1997).

In this work we have estimated the ^{210}Pb deposition flux from total ^{210}Pb and not from the direct atmospheric ^{210}Pb ($^{210}Pb_e$). The two values differ by 6%.

For ^{241}Pu estimates based on ^{241}Am measurements, we have assumed a zero value of ^{241}Am at the time of deposition. In fact the real zero value is the detonation time about 1.5 year earlier. The resulting error is less than 10%.

The greatest source of dispersion between measured and estimated values is the lack of representativeness of the snow samples. Local topography (dunes, sastrugis) and drifting of the snow are very present in Antarctica. For 21 stations, the ^{137}Cs budget is less than the estimated dry deposition, revealing local partial erosion of the deposited snow. At Vostok station, the roughness of the snow surface is equivalent to five yrs of deposition (30 cm), centered around 1965 and representing 40% of the ^{137}Cs budget. This could explain the two different ^{137}Cs budgets observed at this location.

Due to the very short duration of ^{241}Pu deposition, this radionuclide will be more affected by this phenomenon. This could explain the differences between ^{241}Pu deposition at several stations.

The irregular geographical distribution of the measured points does not allow us to establish reliable equidensity scatter plots. For example, to validate the estimated deposition values between Terra Nova and Dumont d'Urville, more samples are necessary (Fig. 3).

The mean deposition of ^{137}Cs in Antarctica obtained from data in the literature is clearly lower than the values estimated (240–260 Bq m^{-2}) from soils sampled on South Shetland Island (60° lat. S) by Roos et al. (1994) and Godoy et al. (1998). Similarly, deposition values published by UNSCEAR (1982) indicate 300, 180 and 70 Bq m^{-2} for latitudes from 60 to 70° S, 70 to 80° S and 80 to 90° S, respectively. Previous values seem to overestimate ^{137}Cs deposition in Antarctica. The limited

number of samples and related values used to calculate these deposition values could be the main reason for the difference between their estimations and our results. With an area of 13,500,000 km^2 and a median value of 56 Bq m^{-2}, the total deposition of ^{137}Cs over Antarctica is estimated at 760 TBq, representing less than 0.08% of the total worldwide deposition of this radionuclide. ^{137}Cs and ^{210}Pb transported in the stratosphere represent excellent atmospheric tracers and could be used to estimate the deposition of other sources of pollution (heavy metals, pesticide, etc.) found in Antarctica.

Acknowledgements

The authors are grateful to all colleagues who participated in field work and sampling operations. Thanks are also due to C. Vincent (LGGE) for his help in the preparation of this paper and to J. Ras (Marine station, LPCM), and Harvey Harder for her help in improving the English.

References

Bendezu, A.M., 1978. Application des mesures de plomb 210 et Sr-90 à l'étude des échanges entre l'atmosphère et la calotte Antarctique. PhD thesis, Université de Paris.

Crozaz, G., 1967. Mise au point d'une méthode de datation des glaciers basée sur la radioactivité du Pb-210. Thèse de doctorat, Université libre de Bruxelles.

Crozaz, G., 1969. Fission products in antarctic snow: an additional reference level in January 1965. Earth Planet. Sci. Let., 6 (1), 6–8.

Cutter, G.A., Bruland, K.W., Risebrough, R.W., 1979. Deposition and accumulation of plutonium isotopes in Antarctica. Nature 279, 628–629.

Delmas, R., Pourchet, M., 1977. Utilisation des filtres échangeurs d'ions pour l'étude de l'activité β globale d'un carottage glaciologique. IAHS Publ 118, 159–163.

Feely, H.W., Seitz, H., Lagomarsino, R.J., Biscaye, P.E., 1966. Transport and fallout of stratospheric radioactive debris. Tellus 18 (2–3), 316–328.

Godoy, J.M., Schuch, L.A., Nordemann, D.J.R., Reis, V.R.G., Ramalho, M., Recio, J.C., Brito, R.R.A., Olech, M.A., 1998. ^{137}Cs, ^{226,228}Ra, ^{210}Pb and ^{40}K concentrations in Antarctic soils, sediment and selected moss and lichen samples. J. Environ. Radioactivity 41 (1), 33–45.

Isaksson, E., Van Den Broeke, M.R., Winther, J.G., Karlof, L., Pinglot, J.F., Gundestrup, N., 1999. Accumulation and proxy-temperature variability in Dronning Maud Land, Antarctica, determined from shallow firn cores. Annals of Glaciology 29, 17–22.

Jouzel, J., Merlivat, L., Pourchet, M., Lorius, C., 1979. A continuous record of artificial tritium fallout at the south pole. Earth Planet. Sci. Lett. 45, 188–200.

Koide, M., Goldberg, E.D., Herron, M.M., Langway, C.C., 1979. Deposition history of artificial radionuclides in the Ross Ice Shelf, Antarctica. Earth Planet. Sci. Lett. 44, 205–223.

Lambert, G., Ardouin, B., Lorius, C., Pourchet, M., 1977. Accumulation of snow and radioactive debris in Antarctica: a possible refined radiochronology beyond reference levels. IAHS Publ. 118, 146–158.

Lambert, G., Ardouin, B., Mesbah-Bendezu, A., 1983. Atmosphère to snow transfert in antarctica. In: Pruppacher, H.R., Semonin, R.G., Slinn, W.G.N. (Eds.), Precipitation Scavenging, Dry Deposition, and Resuspension. New York, Elsevier Science Publishers, pp. 1289–1300.

Nijampurkar, V.N., Rao, D.K., 1993. Polar fallout radionuclides ^{32}Si, ^{7}Be and ^{210}Pb and past accumulation rate of ice at Indian Station, Dakshin Gangotri, East antarctica. J. Environ. Radioactivity 21, 107–117.

Picciotto, E., Wilgain, S., 1963. Fission products in Antarctic snow, a reference level for measuring accumulation. J. Geophys. Res. 68 (21), 5965–5972.

Picciotto, E., Crozaz, G., 1971. Accumulation on the south pole-queen Maud Land traverse, 1964–1968. Antarctic Snow and Ice studies II in Antarctic Research Series 16, 257–315.

Pinglot, J.F., Pourchet, M., 1979. Low level Beta counting with an automatic sample changer. Nuclear Instruments and Methods 166, 483–490.

Pinglot, J.F., Pourchet, M., 1994. Spectrométrie gamma à très bas niveau avec anti- Compton NaI (TI) pour l'étude des glaciers et des sédiments. Note CEA-N-2756, ISSN 0429-3460.

Pinglot, J.F., Pourchet, M., 1995. Radioactivity measurements applied to glaciers and lake sediments. Sci. Total Environ. 173/174, 211–223.

Pinglot, J.F., Pourchet, M., Lefauconnier, B., Hagen, J.O., Isaksson, E., Vaikmac, R., Lamiyama, K., 1999. Accumulation in Svalbard glaciers deduced from ice cores with nuclear tests and Chernobyl reference layers. Polar Research 18 (2), 315–321.

Pourchet, M., Pinglot, J.F., Lorius, C., 1983. Some meteorological applications of radioactive fallout measurements in Antarctic snows. J. Geophys. Res. 88 (C10), 6013–6020.

Pourchet, M., Bartaya, S.K., Maignan, M., Jouzel, J., Pinglot, J.F., Aristarain, A.J., Furdada, G., Kotlyakov, V.M., Mosley-Thompson, E., Preiss, N., Young, N.W., 1997. Distribution and fall-out of ^{137}Cs and other radionuclides over Antarctica. J. Glaciology 43 (45), 435–445.

Roos, P., Holm, E., Persson, R.B.R., Aarkrog, A., Nielsen, S.P., 1994. Deposition of ^{210}Pb, ^{137}Cs, $^{239+240}$Pu, ^{238}Pu, and ^{241}Am in the Antarctic Peninsula area. J. Environ. Radioactivity 24, 235–251.

Sanak, J., 1983. Contribution à l'étude du transport des aérosols d'origine continentale vers l'antarctique. Thèse de doctorat, Université pierre et Marie Curie, Paris.

United Nations Scientific Committee on the effects of Atomic Radiation, UNSCEAR, 1982. Sources, effects and risks of ionizing radiation. United Nations, New York.

Vickers, W.W., 1963. Geochemical dating techniques applied to Antarctic snow samples. General Assembly, Berkeley, August 1963. Intern. Assoc. Sci. Hydrol. Publ. 61, 199–215.

Wilgain, S., Picciotto, E., de Breuck, W., 1965. Strontiumout 90 fallout in Antarctica. J. Geophys. Res. 70 (24), 6023–6032.

Woodward, R.N., 1964. Strontiun 90 and Caesium 137 in Antarctic snows. Nature 204, 1291.